

Inelastic carrier lifetime in graphene

 E. H. Hwang,¹ Ben Yu-Kuang Hu,^{2,1} and S. Das Sarma¹
¹*Condensed Matter Theory Center, Department of Physics, University of Maryland, College Park, Maryland 20742-4111, USA*
²*Department of Physics, University of Akron, Akron, Ohio 44325-4001, USA*

(Received 15 August 2007; published 26 September 2007)

We consider hot-carrier inelastic scattering due to electron-electron interactions in graphene as functions of carrier energy and density. We calculate the imaginary part of the zero-temperature quasiparticle self-energy for doped graphene utilizing the G_0W and random phases approximations. Using the full dynamically screened Coulomb interaction, we obtain the inelastic quasiparticle lifetimes and associated mean free paths. The linear dispersion of graphene gives lifetime energy dependences that are qualitatively different from those of parabolic-band semiconductors. We also get good agreement with data from angle-resolved photoemission spectroscopy experiments.

 DOI: [10.1103/PhysRevB.76.115434](https://doi.org/10.1103/PhysRevB.76.115434)

PACS number(s): 81.05.Uw, 71.10.-w, 71.18.+y, 73.63.Bd

I. INTRODUCTION

Graphene, a single layer of carbon atoms covalently bonded together in a honeycomb structure (as in a monolayer of graphite), was previously thought to be unstable and hence nonexistent in a free state. Recently, however, Novoselov *et al.* reported¹ that they had succeeded in fabricating single graphene sheets. Subsequently, several experimental groups have reported interesting transport and spectroscopic measurements,²⁻⁴ which has led to rapidly burgeoning experimental and theoretical interest in this field.

The overlap of the π_z orbitals between neighboring carbon atoms in the graphene plane is accurately described by a tight-binding Hamiltonian. Around the K and K' points (often called Dirac points) which are at the corners of the hexagonal Brillouin zone, the kinetic energy term of the Hamiltonian is well approximated by a two-dimensional (2D) Dirac equation for massless particles, $\hat{H}_0 = -v_0(\sigma_x \hat{k}_x + \sigma_y \hat{k}_y)$, where σ_x and σ_y are 2×2 Pauli spinors and \mathbf{k} is the momentum relative to the Dirac points ($\hbar = 1$ throughout this paper). The two components of the spinors correspond to occupancy of the two sublattices of the honeycomb structure in a hexagonal lattice. This \hat{H}_0 gives a linear energy dispersion relation $\epsilon_{k,s} = sv_0|\mathbf{k}|$, where $s = +1$ (-1) for the conduction (valence) band. The corresponding density of states (DOS) is $D(\epsilon) = g_s g_v |\epsilon| / (2\pi v_0^2)$, where $g_s = 2$ and $g_v = 2$ are the spin and valley (i.e., K and K' points) degeneracies, respectively. Thus, graphene is a gapless semiconductor. In intrinsic graphene, the Fermi level lies at the Dirac points, but as with other semiconductors it is possible to shift the Fermi level by either doping the sample or applying an external gate voltage, which introduces 2D free carriers (electrons or holes) producing extrinsic graphene with gate-voltage-induced tunable carrier density. The Fermi momentum (k_F) and the Fermi energy (E_F , relative to the Dirac point energy) of graphene are given by $k_F = (4\pi n / g_s g_v)^{1/2}$ and $|E_F| = v_0 k_F$ where n is the 2D carrier (electron or hole) density.

Interparticle interactions can significantly affect electronic properties, particularly in systems of reduced dimensionality. Moreover, the linear energy dispersion around the Dirac points gives condensed matter experimentalists a unique opportunity to study interaction effects on effectively massless

particles. In this paper, we focus on the effect of electron-electron ($e-e$) interaction effects on the imaginary part of quasiparticle self-energies, $\text{Im}[\Sigma]$. From $\text{Im}[\Sigma]$, we can extract the quasiparticle lifetime, which gives information that is relevant both to fundamental questions, such as whether or not the system is a Fermi liquid, and to possible applications, such as the energy dissipation rate of injected carriers in a graphene-based device. In particular, an important physical quantity of both fundamental and technological significance is the hot-carrier mean free path, which we calculate as a function of energy, density, and in-plane dielectric constant. Furthermore, $\text{Im}[\Sigma]$, being the width of the quasiparticle spectral function, is related to measurements in angle-resolved photoemission spectroscopy (ARPES).

The rest of the paper is organized as follows. In Sec. II we discuss the general theory of the self-energy of graphene. In Sec. III we present our calculated quasiparticle damping rate of graphene and compare with the damping rate of parabolic 2D systems. In Sec. IV we show the detail results of the self-energy, and finally we conclude in Sec. V.

II. THEORY

We evaluate the self-energy Σ within the leading-order ring-diagram G_0W approximation, which is appropriate for weak-coupling systems, given by⁵

$$\begin{aligned} \Sigma_s(\mathbf{k}, i\omega_n) = & -k_B T \sum_{s'} \sum_{q, i\nu_n} G_{0,s'}(\mathbf{k} + \mathbf{q}, i\omega_n + i\nu_n) \\ & \times W(q, i\nu_n) F_{ss'}(\mathbf{k}, \mathbf{k} + \mathbf{q}). \end{aligned} \quad (1)$$

Here, T is temperature, $s, s' = \pm 1$ are band indices, G_0 is the bare Green's function, ω_n and ν_n are Matsubara fermion and boson frequencies, respectively, W is the screened Coulomb interaction, and $F_{ss'}(\mathbf{k}, \mathbf{k}') = \frac{1}{2}(1 + ss' \cos \theta_{\mathbf{k}\mathbf{k}'})$, where $\theta_{\mathbf{k}\mathbf{k}'}$ is the angle between \mathbf{k} , \mathbf{k}' , arises from the overlap of $|s\mathbf{k}\rangle$ and $|s'\mathbf{k}'\rangle$. The screened interaction $W(q, i\nu_n) = V_c(q) / \epsilon(q, i\nu_n)$, where $V_c(q) = 2\pi e^2 / \kappa q$ is the bare Coulomb potential (κ = background dielectric constant) and $\epsilon(q, i\nu_n)$ is the 2D dynamical dielectric function. In the random phase approximation, $\epsilon(q, i\nu_n) = 1 - V_c(q) \Pi_0(q, i\nu_n)$, where the irreducible

polarizability Π_0 is approximated by the bare bubble diagram,^{6,7} which gives the familiar Lindhard expression [with a modification to include the form factor $F_{ss'}(\mathbf{k}, \mathbf{k}')$].

The self-energy approximation described by Eq. (1) should be an excellent approximation for graphene since graphene is inherently a weak-coupling (or “high-density” in parabolic-band systems) 2D system.⁸ The measure of the ratio of the potential to the kinetic energy in graphene is $r_s = e^2 / (\kappa v_0) \approx 2.2 / \kappa$, where κ is the effective dielectric constant of the graphene layer and the media surrounding it. (Note that, unlike regular parabolic-band systems, r_s in graphene does not depend on density.) Typically, in graphene, $r_s < 1$, implying that the system is in the weak-coupling regime.

After the standard procedure of analytical continuation from $i\omega_n$ to $\omega + i0^+$, the retarded self-energy can be separated into the exchange and correlation parts $\Sigma_s^{\text{ret}}(\mathbf{k}, \omega) = \Sigma_s^{\text{ex}}(\mathbf{k}) + \Sigma_s^{\text{cor}}(\mathbf{k}, \omega)$.⁵ The exchange part is given by

$$\Sigma_s^{\text{ex}}(\mathbf{k}) = - \sum_{s' \mathbf{q}} n_F(\xi_{\mathbf{k}+\mathbf{q},s'}) V_c(\mathbf{q}) F_{ss'}(\mathbf{k}, \mathbf{k} + \mathbf{q}), \quad (2)$$

where n_F is the Fermi function and $\xi_{k,s} = \epsilon_{k,s} - \mu$ is the electron energy relative to the chemical potential μ . This term in graphene is discussed in Ref. 9. At typical experimental densities, the Fermi temperature $T_F \equiv |E_F| / k_B$ in graphene is very high compared to the temperature of the sample (e.g., for $n = 10^{13} \text{ cm}^{-2}$, $T_F \approx 3.1 \times 10^3 \text{ K}$, and $T_F \propto \sqrt{n}$). Therefore, it is an excellent approximation to set the temperature $T = 0$, which we do in the rest of this paper. This implies that $n_F(\xi_{\mathbf{k},s}) = \theta(\xi_{\mathbf{k},s})$ (where θ is Heaviside unit step function) and $\mu = E_F$.

The correlation part $\Sigma_s^{\text{cor}}(\mathbf{k}, \omega)$ is defined to be the part of $\Sigma_s^{\text{ret}}(\mathbf{k}, \omega)$ not included in $\Sigma_s^{\text{ex}}(\mathbf{k})$. In the G_0W approximation, the $\Sigma_s^{\text{cor}}(\mathbf{k}, \omega)$ can be decomposed into the line and pole contributions $\Sigma_s^{\text{cor}} = \Sigma_s^{\text{line}} + \Sigma_s^{\text{pole}}$,¹⁰ where

$$\Sigma_s^{\text{line}}(\mathbf{k}, \omega) = - \sum_{s' \mathbf{q}} \int_{-\infty}^{\infty} \frac{d\omega'}{2\pi} \frac{V_c(\mathbf{q}) F_{ss'}(\mathbf{k}, \mathbf{k} + \mathbf{q})}{\xi_{\mathbf{k}+\mathbf{q},s'} - \omega - i\omega'} \times \left[\frac{1}{\epsilon(q, i\omega')} - 1 \right], \quad (3)$$

$$\Sigma_s^{\text{pole}}(\mathbf{k}, \omega) = \sum_{s' \mathbf{q}} [\theta(\omega - \xi_{\mathbf{k}+\mathbf{q},s'}) - \theta(-\xi_{\mathbf{k}+\mathbf{q},s'})] \times V_c(\mathbf{q}) F_{ss'}(\mathbf{k}, \mathbf{k} + \mathbf{q}) \left[\frac{1}{\epsilon(q, \xi_{\mathbf{k}+\mathbf{q},s'} - \omega)} - 1 \right]. \quad (4)$$

The Σ_s^{ex} and Σ_s^{line} are completely real, the latter because $\epsilon(q, i\omega)$ is real. Thus, $\text{Im}[\Sigma_s^{\text{pole}}(\mathbf{k}, \omega)]$ gives the total contribution to the imaginary part of the self-energy—i.e.,

$$\text{Im}[\Sigma_s^{\text{ret}}(\mathbf{k}, \omega)] = \sum_{s'} \int \frac{d\mathbf{q}}{(2\pi)^2} [\theta(\omega - \xi_{\mathbf{k}+\mathbf{q},s'}) - \theta(-\xi_{\mathbf{k}+\mathbf{q},s'})] \times V_c(q) \text{Im} \left[\frac{1}{\epsilon(q, \xi_{\mathbf{k}+\mathbf{q},s'} - \omega)} \right] F_{ss'}(\mathbf{k}, \mathbf{k} + \mathbf{q}). \quad (5)$$

The inverse quasiparticle lifetime (or, equivalently, the scattering rate) $\Gamma_s(\mathbf{k})$ of state $|s\mathbf{k}\rangle$ is obtained by setting the frequency in imaginary part of the self-energy to the on-shell (bare quasiparticle) energy $\xi_{s\mathbf{k}}$ —i.e.,

$$\Gamma_s(\mathbf{k}) = 2 \text{Im}[\Sigma_s^{\text{ret}}(\mathbf{k}, \xi_{s\mathbf{k}})]. \quad (6)$$

(The factor of 2 comes from the squaring of the wave function to obtain the occupation probability.) The G_0W self-energy approximation used here is equivalent to the Born approximation for the scattering rate. Note that the integrand of Eq. (5) is nonzero only when $\text{Im}[\epsilon] \neq 0$ or $\text{Re}[\epsilon] = 0$. These correspond to scattering off single-particle excitations and plasmons, respectively.

III. QUASIPARTICLE SCATTERING RATE

The self-energies and quasiparticle lifetimes of graphene and conventional parabolic-band semiconductors differ considerably. These differences can be explained with the help of Fig. 1, which shows the single-particle excitation (SPE) and injected-electron energy loss (IEEL) continua and the plasmon dispersion for a direct gapless 2D parabolic-band semiconductor and for graphene. The intersections of the IEEL continua with the SPE continua and the plasmon dispersion lines indicate allowed decay processes via $e-e$ interactions. In both doped parabolic-band semiconductors and graphene, an injected electron will decay via single-particle intraband excitations of electrons in the conduction band. In parabolic-band semiconductors, an electron injected with sufficient kinetic energy can also decay via plasmon emissions and interband SPE (also known as “impact ionization”). On the other hand, as shown in Fig. 1(b), electrons injected into doped graphene cannot decay via plasmon emission and the region in $q-\omega$ where decay via interband SPE is allowed [along the straight line segment between $\omega = v_0 k_F$ and $v_0(k - k_F)$, for $k > 2k_F$] is of measure zero. In fact, within the Born approximation the quasiparticle lifetime of undoped graphene due to $e-e$ interactions at $T = 0$ is infinite. (Multiparticle excitations, which are excluded in the approximations used here, will give a quasiparticle a finite lifetime,¹¹ but this is a relatively small effect in graphene.)

In doped graphene, the only independent parameters relevant for Born-approximation quasiparticle scattering rates at $T = 0$ are the Fermi energy relative to the Dirac point $E_F = v_0 k_F$ and the dimensionless coupling constant $r_s = e^2 / (\kappa v_0)$. The scattering rate, which has units of energy, must therefore be proportional to E_F and must be a function only of $\epsilon / E_F = k / k_F$ and r_s . Figure 2(a) shows the Born-approximation $T = 0$ quasiparticle lifetime $1/\tau = \Gamma$ due to $e-e$ interactions as a function of energy $\xi(k) = \epsilon_k - E_F$. Since the speed of the quasiparticles close the Dirac points is approxi-

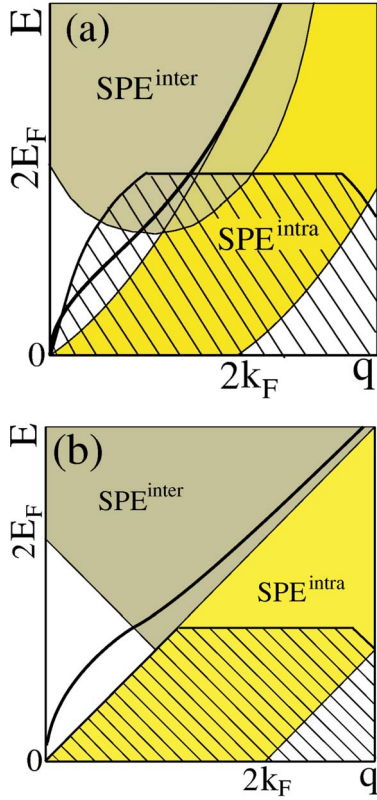


FIG. 1. (Color online) The single-particle excitations (intra- and interband) and injected-particle energy-loss (hatched region) continua, and plasmon dispersion (thick line) for (a) gapless parabolic-band semiconductor with equal hole and electron masses and (b) graphene, at $T=0$ with Fermi energy in the conduction band. For gapped semiconductors, the interband continua are shifted up by the energy gap.

mately a constant $v_0 \approx 10^8$ cm/s, the inelastic mean free path ℓ is obtained by $\ell(\xi) = v_0 \tau(\xi)$. In Fig. 2(b), we provide the corresponding ℓ , which shows that at $n = 10^{13}$ cm $^{-2}$ a hot electron injected with an energy of 1 eV above E_F has an ℓ due to e - e interactions that is on the order of 40 nm. This will have implications for designing any hot-electron transistor-type graphene devices. In particular, because Klein tunneling¹² in graphene creates problems in the standard gate-potential switching method in transistors, in its place could be a switch based on modulating the electron energy ξ in a regime where $|\partial\ell/\partial\xi|$ is large.

As with doped parabolic-band 2D semiconductors,^{13–15} in graphene $\Gamma(k) = 1/\tau(k) \propto (k - k_F)^2 |\log(|k - k_F|)|$ for $k \approx k_F$ due to scattering phase-space restrictions. Farther away from k_F , however, the dependences of Γ on k in graphene and in parabolic-band semiconductors are markedly and qualitatively different. To wit, in parabolic-band semiconductors plasmon emission^{14,16} and interband collision thresholds¹⁷ cause discontinuities in the $\Gamma(k)$, as shown in Fig. 2(c), but the graphene $\Gamma(k)$ is a smooth function because both plasmon emission and interband processes are absent.

IV. SELF-ENERGY

In order to see the effects of the plasmons and interband SPE in graphene in $\text{Im}[\Sigma^{\text{ret}}]$, one must look *off shell*—i.e.,

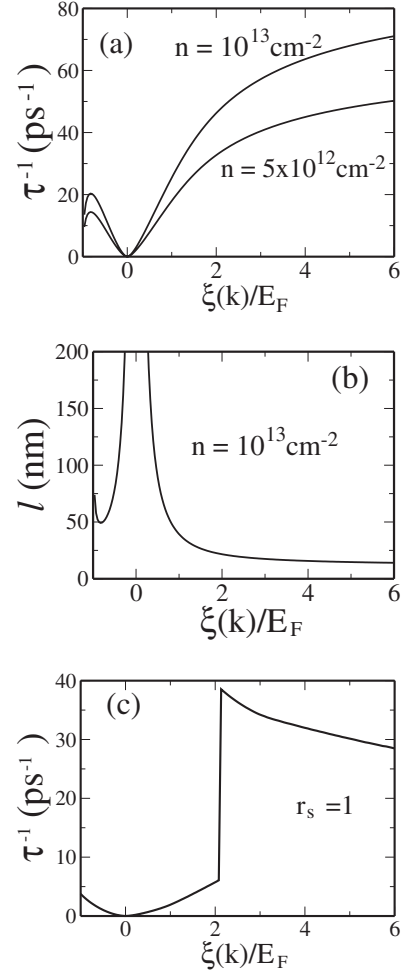


FIG. 2. (a) Inelastic quasiparticle lifetime/scattering rate ($1/\tau = \Gamma$) in graphene due to dynamically screened e - e interactions, as a function of energy at $T=0$ for different densities, within the Born approximation. (b) The corresponding quasiparticle mean free path for $n = 10^{13}$ cm $^{-2}$ (corresponding to $E_F \approx 0.4$ eV). (c) Equivalent scattering rate for a parabolic-band semiconductor (without interband processes), for comparison.

$\omega \neq \xi_{k,s}$. The off-shell $\text{Im}[\Sigma_s^{\text{ret}}]$ is not merely of academic interest; it is needed to interpret data from ARPES. The spectra of the ARPES electrons ejected from graphene give the electronic spectral function, from which one can infer $\Sigma_s^{\text{ret}}(\mathbf{k}, \omega)$.¹⁸ Physically, in the G_0W approximation, the off-shell $2 \text{Im}[\Sigma_s^{\text{ret}}(\mathbf{k}, \omega)]$ gives the Born-approximation decay rate of the quasiparticle in state \mathbf{k} if it had kinetic energy $\omega + E_F$ rather than $\xi_{\mathbf{k}} + E_F$.

In Fig. 3 we show $\text{Im}[\Sigma_+^{\text{ret}}(k, \omega)]$ for $k=0$ and $k=k_F$ as a function of ω . Within the G_0W approximation, the contributions to the off-shell $\text{Im}[\Sigma_s^{\text{ret}}(\mathbf{k}, \omega)]$ can be visualized as the intersection of the SPE continuum and plasmon line in Fig. 1 with the vertically displaced IEEL.¹⁹ At $k=0$ there are two contributions to $\text{Im}[\Sigma]$: the intraband and interband SPEs. For low energies ($|\omega| \lesssim E_F$) only intraband SPE contributes to $\text{Im}[\Sigma]$. Its contribution reaches a maximum around Fermi energy, then decreases gradually with increasing energy, as is the case with a parabolic-band semiconductor¹⁶ where it is

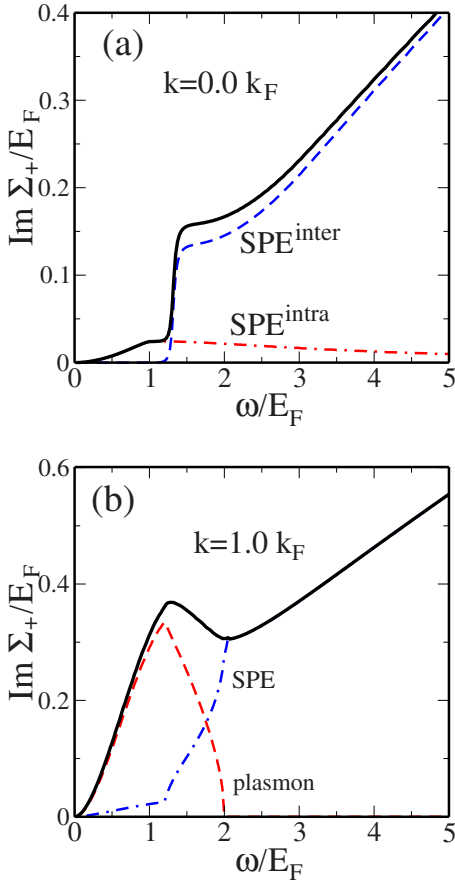


FIG. 3. (Color online) The imaginary part the retarded self-energy at $T=0$ (thick line) for (a) $k=0$ and (b) $k=k_F$ as a function of energy. The dot-dashed and dashed lines in (a) are the $\text{SPE}^{\text{intra}}$ and $\text{SPE}^{\text{inter}}$ contributions, respectively. The dot-dashed and the dashed lines in (b) are the total SPE (intraband and interband SPE) and the plasmon contributions, respectively.

the only decay channel for the quasiparticle (assuming $\omega < \text{band gap energy}$). But in graphene there is a new decay channel of the quasiparticle: the interband SPE. Due to the phase-space restrictions, the interband SPE does not contribute to the self-energy at low energies, but at higher energies ($\omega \geq E_F$) its contribution increases sharply, overwhelming the $\text{SPE}^{\text{intra}}$ contribution. The $\text{SPE}^{\text{inter}}$ contribution then increases almost linearly with ω , with the same slope as for intrinsic graphene.⁸ Plasmons do not contribute to $\text{Im}[\Sigma_+^{\text{ret}}(\mathbf{k}=0, \omega)]$ for $\omega > 0$.

At $k=k_F$, not only do plasmons contribute to $\text{Im}[\Sigma]$, in the low-energy ($\omega \leq 2E_F$) regime, they actually dominate over the SPE contributions, as can be seen in Fig. 3(b). In contrast, in parabolic-band 2D electron gases (2DEGs) the plasmon and SPE contributions to $\text{Im}[\Sigma^{\text{ret}}(k_F, \omega)]$ go as ω^2 and $\omega^2 \ln \omega$, respectively,¹⁴ and hence both contributions are roughly equal in magnitude.

Figure 4 shows the imaginary part of the quasiparticle self-energies for the conduction band, $\text{Im}[\Sigma_+^{\text{ret}}]$, and the valence band, $\text{Im}[\Sigma_-^{\text{ret}}]$, of graphene for several different wave vectors. For $k > k_F$, the $\text{Im}[\Sigma_+^{\text{ret}}]$ shows a sharp peak associated with the plasmon emission threshold. In the high-energy

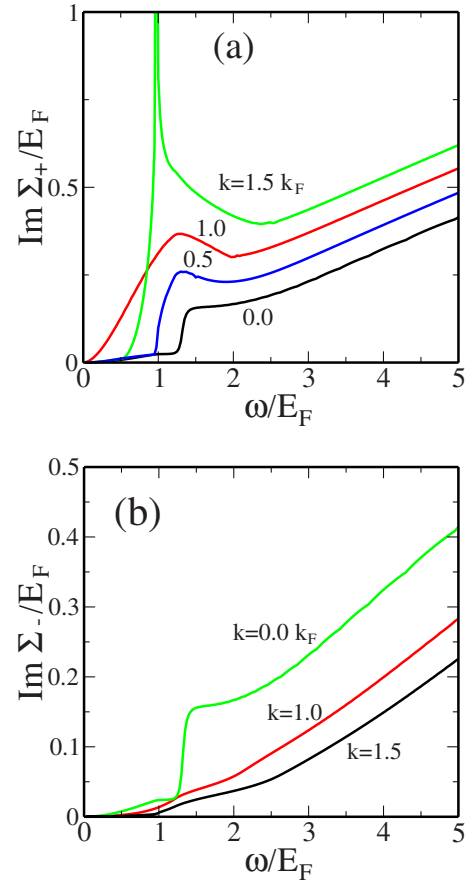


FIG. 4. (Color online) The imaginary part of the self-energy as a function of energy for wave vectors $k=(0, 0.5, 1.0, 1.5)k_F$ for (a) the conduction band and (b) the valence band of electron-doped graphene at $T=0$.

regime, the dominant contribution to $\text{Im}[\Sigma]$ comes from the interband SPE, which gives rise to an $\text{Im}[\Sigma]$ which is linear in ω for all wave vectors. Note that within the G_0W approximation, for a given r_s in graphene, the Σ , ω , and k scale with E_F , E_F , and k_F , respectively; i.e., for fixed r_s , the function $\tilde{\Sigma}(\tilde{k}, \tilde{\omega})$ is universal, where $\tilde{\Sigma}=\Sigma/E_F$, $\tilde{k}=k/k_F$, and $\tilde{\omega}=\omega/E_F$.

Finally, Fig. 5 shows the calculated $\text{Im}[\Sigma_+^{\text{ret}}]$ at fixed $k=k_F$ as a function of energy ω for various densities. *No fitting parameters were used* in this calculation. These results compare favorably with the recent data from ARPES experiments by Bostwick *et al.*³ from which they extract $\text{Im}[\Sigma^{\text{ret}}(k_F, \omega)]$ for different densities. (The overall scale is different because we have assumed a SiO_2 substrate used by some other groups, whereas the samples of Ref. 3 were on SiC, which has a different κ .) Bostwick *et al.* invoked plasmons, SPE, and phonon effects in interpreting their data. We find that including just the plasmon and SPE effects, we get reasonable agreement with their data, except for features near 0.2 eV which probably can be explained by calculations that include electron-phonon interactions.

Before concluding, we discuss some of the approximations that lead to Eq. (1). We ignore on-site (Hubbard) $e-e$ interactions because, at zero magnetic field, this interaction

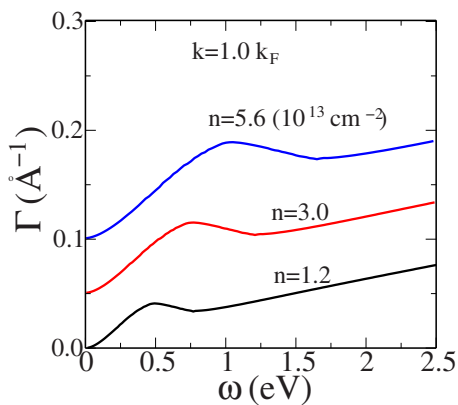


FIG. 5. (Color online) Scattering rate as a function of energy for different densities $n = 1.2, 3.0, 5.6 \times 10^{13} \text{ cm}^{-2}$ (for clarity, successive lines are shifted upward by 0.05 \AA^{-1}), in the form of Fig. 3 of Bostwick *et al.* (Ref. 3).

is irrelevant in the renormalization group sense.²⁰ Our calculation *does* include both intraband and interband scattering processes, since our expression for $\Sigma_s(\mathbf{k}, i\omega_n)$, Eq. (1), contains a pseudospin sum $s' = \pm 1$. Finally, there is an issue about the coupling of the bands due to interactions; i.e., because of nondiagonal terms $\Sigma_{ss'}$ with $s \neq s'$, the elementary excitations are a superposition of states from the conduction and valence bands. Dyson's equation in this case is $\mathbf{G}^{-1} = \mathbf{G}_0^{-1} - \Sigma$, where the quantities are 2×2 matrices, which, when written out in full, is

$$\mathbf{G}^{-1}(\mathbf{k}, \omega) = \begin{pmatrix} \omega - \xi_+(k) - \Sigma_{++}(\mathbf{k}, \omega) & -\Sigma_{+-}(\mathbf{k}, \omega) \\ -\Sigma_{-+}(\mathbf{k}, \omega) & \omega - \xi_-(k) - \Sigma_{--}(\mathbf{k}, \omega) \end{pmatrix}. \quad (7)$$

The excitation energies are given by the poles of \mathbf{G} , or equivalently, the zeros of the determinant of \mathbf{G}^{-1} . Our calculation is equivalent to ignoring the off-diagonal terms

$\Sigma_{+-}\Sigma_{-+}$ in the determinant of \mathbf{G}^{-1} . The off-diagonal terms $\Sigma_{\pm\mp}$ are each of order r_s , and therefore the product $\Sigma_{+-}\Sigma_{-+} \sim r_s^2$ which can be ignored in the weak-coupling regime. We also ignore intervalley scattering because the Born-approximation Coulomb scattering rate in 2D is $\propto q^{-2}$, implying that small- q intravalley scattering processes dominate over the large- q intervalley ones.

V. CONCLUSION

To conclude, we have calculated the electron-electron interaction induced hot-electron inelastic scattering in graphene, finding a number of intriguing and significant differences with the corresponding 2D parabolic dispersion systems. Our infinite ring-diagram G_0W approximation should be an excellent quantitative approximation for graphene since graphene is a low- r_s (i.e., weak-coupling) system. Our $T=0$ results should remain for $T \ll T_F$, which is typically the case in experiments. We obtain good agreement with recent ARPES data without invoking any phonon effects. ARPES data has recently created a controversy with respect to the role of plasmons.^{3,4} Our detailed calculation using a realistic model generally agrees with the interpretation of the data in Ref. 3. The calculated inelastic scattering length ℓ as a function of energy ξ is by itself of interest in the context of ballistic hot-electron transistor applications of graphene, where the performance limitation is inelastic scattering. Furthermore, the Klein tunneling effect in graphene makes it difficult to switch transistors by a gate-voltage-induced depletion [as in a conventional metal-oxide-semiconductor field-effect transistor (MOSFET)]. In its place, one could imagine a graphene-based transistor in which switching is achieved by modulation of the injection carrier energy in the regime of ξ where $|d\ell(\xi)/d\xi|$ is large.

ACKNOWLEDGMENT

This work is supported by the U.S. ONR.

¹K. S. Novoselov, A. K. Geim, S. V. Morozov, D. Jiang, Y. Zhang, S. V. Dubonos, I. V. Grigorieva, and A. A. Firsov, *Science* **306**, 666 (2004); *Nature (London)* **438**, 197 (2005).

²See, e.g., C. Berger, Z. Song, T. Li, X. Li, A. Y. Ogbazghi, R. Feng, Z. Dai, A. N. Marchenkov, E. H. Conrad, P. N. First, and W. A. de Heer, *J. Phys. Chem. B* **108**, 19912 (2004); Y. Zhang, Y.-W. Tan, H. L. Stormer, and P. Kim, *Nature (London)* **438**, 201 (2005); J. S. Bunch, Y. Yaish, M. Brink, K. Bolotin, and P. L. McEuen, *Nano Lett.* **5**, 2887 (2005); A. K. Geim and K. S. Novoselov, *Nat. Mater.* **6**, 183 (2007), and references therein.

³A. Bostwick, T. Ohta, T. Seyller, K. Horn, and E. Rotenberg, *Nat. Phys.* **3**, 36 (2007).

⁴S. Y. Zhou, G.-H. Gweon, J. Graf, A. Fedorov, C. Spataru, R. Diehl, Y. Kopelevich, D.-H. Lee, S. G. Louie, and A. Lanzara, *Nat. Phys.* **2**, 595 (2006).

⁵See, e.g., G. D. Mahan, *Many Particle Physics*, 3rd ed. (Kluwer/Plenum, New York, 2000).

⁶E. H. Hwang and S. Das Sarma, *Phys. Rev. B* **75**, 205418 (2007).

⁷Kenneth W.-K. Shung, *Phys. Rev. B* **34**, 979 (1986).

⁸S. Das Sarma, E. H. Hwang, and W.-K. Tse, *Phys. Rev. B* **75**, 121406(R) (2007).

⁹E. H. Hwang, Ben Yu-Kuang Hu, and S. Das Sarma, arXiv:cond-mat/0703499 (unpublished); Yafis Barlas, T. Pereg-Barnea, Marco Polini, Reza Asgari, and A. H. MacDonald, *Phys. Rev. Lett.* **98**, 236601 (2007).

¹⁰John J. Quinn and Richard A. Ferrell, *Phys. Rev.* **112**, 812 (1958).

¹¹J. González, F. Guinea, and M. A. H. Vozmediano, *Phys. Rev. Lett.* **77**, 3589 (1996).

¹²O. Klein, *Z. Phys.* **53**, 157 (1929); M. I. Katsnelson, K. S. Novoselov, and A. K. Geim, *Nat. Phys.* **2**, 620 (2006); J. Milton Pereira, Jr., V. Mlinar, F. M. Peeters, and P. Vasilopoulos, *Phys. Rev. B* **74**, 045424 (2006); V. V. Cheianov and V. I. Fal'ko, *ibid.* **74**, 041403(R) (2006).

¹³A. V. Chaplik, *Zh. Eksp. Teor. Fiz.* **60**, 1845 (1971) [*Sov. Phys.*

- JETP **33**, 997 (1971)]; C. Hodges, H. Smith, and J. W. Wilkins, Phys. Rev. B **4**, 302 (1971).
- ¹⁴G. F. Giuliani and J. J. Quinn, Phys. Rev. B **26**, 4421 (1982).
- ¹⁵Lian Zheng and S. Das Sarma, Phys. Rev. B **53**, 9964 (1996); T. Jungwirth and A. H. MacDonald, *ibid.* **53**, 7403 (1996).
- ¹⁶R. Jalabert and S. Das Sarma, Phys. Rev. B **40**, 9723 (1989).
- ¹⁷L. V. Keldysh, Zh. Eksp. Teor. Fiz. **48**, 1692 (1965) [Sov. Phys. JETP **21**, 1135 (1965)].
- ¹⁸For a review of ARPES, see, e.g., A. Damascelli, Z. Hussain, and Z.-X. Shen, Rev. Mod. Phys. **75**, 473 (2003).
- ¹⁹More accurately, the contributions come from the regions in the E - q plane between $E=0$ and $E=\omega$ in which the SPE and plasmon lines intersect with the energy loss *and* gain spectrum that is shifted along the E axis by $\omega-\xi_k$.
- ²⁰J. González, F. Guinea, and M. A. H. Vozmediano, Phys. Rev. B **63**, 134421 (2001).